

# Lossless Multi-mode Interband Image Compression and its Application in Space Images

Xiaolin Chen, Jose L. Nunez-Yanez and Nishan Canagarajah  
*Department of Electrical and Electronic Engineering*  
*University of Bristol, UK*

*Email: Xiaolin.Chen@bristol.ac.uk, J.L.Nunez-Yanez@bristol.ac.uk, Nishan.Canagarajah@bristol.ac.uk*

## ABSTRACT

This paper presents a novel Lossless Multi-Mode Interband image Compression (LMMIC) scheme and its application in space imagery. The algorithm takes advantage of a multi-mode strategy which uses different coding methods to encode image regions with different features. This strategy is especially suitable for removing interband redundancy. The adaptation of intraband and interband coding further strengthens this algorithm. We also proposed a hardware architecture to support the algorithm. Experimental results show that LMMIC achieves good compression ratios while maintaining low complexity and hence hardware amenability.

## I. INTRODUCTION

Modern multimedia technology generates huge amount of image data, most of which are multispectral images. We define “multispectral images” here as images containing more than one spectral band. For instance, normal colour images have three bands, e.g. red, green and blue (RGB). Some high fidelity image capture systems, e.g. the VASARI imaging system [1] developed at the National Gallery in London, use a seven-channel multispectral camera to capture paintings. In remote sensing, the LANDSAT 7 [2] satellite images have seven spectral bands, and the AVIRIS (Airborne Visible/Infrared Imaging Spectrometer) [3] hyperspectral images contain 224 contiguous bands. In medical imaging, multispectral images, such as magnetic resonance imaging (MRI), also prevail. As many applications demand perfect reconstruction of images, lossless compression on multispectral images is increasingly important.

Before multispectral images received a lot of research attention, gray-scale image compression techniques [4,5,6] were used directly to treat colour images as three independent gray-scale images. However, spectral bands within an image are often correlated, to exploit this correlation is essential for multispectral image compression. Many researchers have applied transform and prediction based techniques for spectral decorrelation. Popular transform based techniques include vector quantization [7,8], discrete wavelet transform [9,10], and vector-lifting [11]. These techniques are effective in removing spectral redundancy, but their high complexity and often joint encoding of several bands (e.g. 16 bands in [10]) are obstacles for hardware implementation and real-time processing. On the other hand, prediction techniques excel with efficiency and simplicity. For instance, the prediction-based Inter-band CALIC [12] is claimed to offer one of the best interband lossless compression results in literature, but it requires complex interband correlation coefficients calculation and context formation. SICLIC [13] is a simple and efficient colour image coder based on LOCO-I [4], but its 3-band joint-run mode, while offering good bit rates, reduces the flexibility of encoding any number of bands.

In this paper we propose a Lossless Multi-Mode Interband image Compression (LMMIC) scheme, aiming at providing efficient lossless multispectral image compression with the capability of real-time processing and hardware amenability, which is highly desirable in practice when data volume is massive and computation becomes resource demanding. The core of this scheme is a new multi-mode strategy, which is inspired by the concept of segmentation. Generally, segmentation is to partition an image into multiple segments in order to change the representation of an image into something meaningful or easy to analyse. Traditional segmentation, e.g. statistical model-based methods and graph-based methods, is often too complex to implement in real-time compression. The novelty of our scheme is to apply the concept of segmentation to group pixels with similar features and use different methods to encode them. We design a new ternary-mode to detect and encode the edges and smooth regions, and use a run-length coder [4] to encode the homogeneous regions, and a regular-mode for the rest of the image, say the texture regions. This strategy is particularly suitable for space images because there are usually larger smooth areas in space images. We also enable the adaptation of interband and intraband prediction in all three modes by applying a new gradient-based switch. The proposed scheme does not only offer good compression ratios, but also the distinctive feature of flexibly encoding any number of bands. As LMMIC only involves a limited number of addition and shifting, it is hardware amenable. Note that the proposed scheme is for general purpose (e.g. space, medical, archiving) images but not specifically geared for hyperspectral images. Since some techniques for hyperspectral images make specific use of the structure of these images, for example, by including a band ordering process [14] or by clustering a number of bands [10], we do not include those highly specialised and not necessarily hardware amenable methods in our comparison study. However, we acknowledge that refining our techniques to cater for hyperspectral images is an interesting topic for further research.

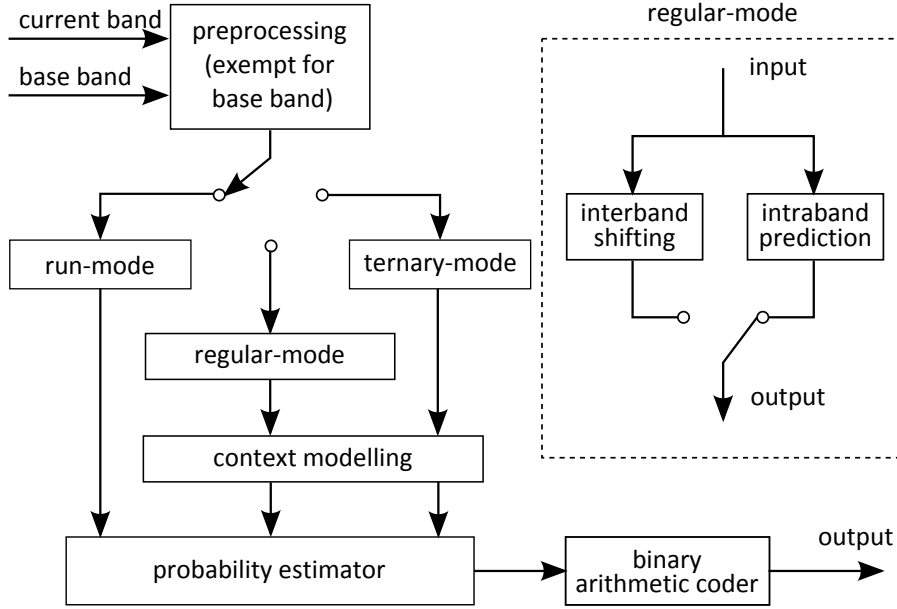


Fig. 1. Schematic of the proposed image compression system

This paper is organized as follows. In Section II we present an overview of LMMIC. Then we explain the core techniques – multi-mode strategy in Section III and band shifting and gradient-based switching in Section IV. The hardware architecture to support LMMIC is presented in Section V. We compare the performance of LMMIC with other state-of-the-art schemes in Section VI and conclude our work in Section VII.

## II. AN OVERVIEW OF LMMIC

An image contains many features, such as smooth regions, edges, texture etc. The complexity of an image is an obstacle for compression, thus segmentation (also referred to as region-based methodology) is a viable approach to help with distinguishing these features. The lossless image compression method TMW [15], which achieves the best gray-scale image compression ratio so far, uses segmentation to analyse the image in the first pass. Shen [16] applied the region-growing algorithm for segmentation of lossless compression of medical images. Ratakonda [17] used multiscale segmentation to encode general images. However, they are all complex two-pass schemes so cannot meet well the real-time processing requirement. Due to the complexity of segmentation, we skip the conventional segmentation methods, but instead propose to apply its concept, by detecting the image features adaptively, and choose suitable modes to encode these features. The function of “segmenting” is achieved by some carefully designed entry conditions into each mode. This is the idea that our scheme is based on.

Fig. 1 shows the schematic of LMMIC. It consists of preprocessing, prediction, context modelling and arithmetic coding. At the beginning, a base band is chosen. It is encoded independently using intraband compression method. Then a preprocessing step is performed on all bands except the base band to calculate the band difference between the current band and the base band. The output of the preprocessing includes a difference band, an original band and a base band. They are then fed into the multi-mode predictor. The prediction step includes run-mode, ternary-mode and regular mode. In each mode, there is a choice between intraband and interband operations. For regular-mode, we proposed a band shifting technique for interband prediction, while the intraband prediction is based on the Gradient Adjusted Predictor (GAP) [5]. A new gradient-based switching is designed to select the better predictor. We also enable adaptation on intraband and interband operations for run-mode and ternary-mode. This multi-mode strategy applies to all bands in an image. The context modelling is constructed in a similar but simpler way as in [5] to further exploit higher order redundancy. The probability estimator and arithmetic coding are designed in a similar way as in [18]. LMMIC offers not only very good compression ratios, but also the distinctive feature of encoding any number of bands, since the structure of our scheme does not enforce any restriction on the number of bands to be coded. The simple multi-mode strategy and switching method make it hardware amenable.

## III. MULTI-MODE STRATEGY

As important as segmenting regions correctly in segmentation, it is crucial to decide under which circumstances the system should be working under which mode, since it is exactly these entry conditions “segmenting” the image. In this

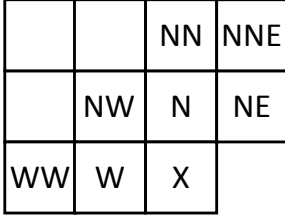


Fig. 2. Neighboring pixels of the current pixel.

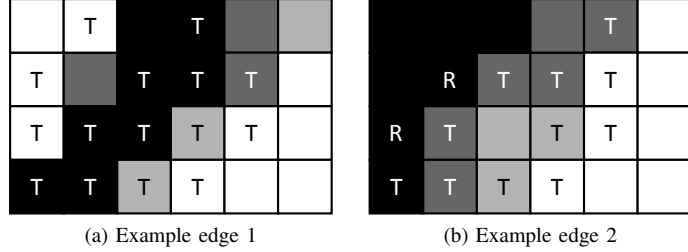


Fig. 3. Areas where ternary-mode is performed.

section, we present how each mode works and the conditions for entering each mode. Prior to that, the preprocessing step is briefly described below.

### A. Preprocessing

In Fig. 1, to start the process, one band is chosen as base band. For instance the band G in RGB images, or the first band received in a multispectral image. The base band is coded with intraband coding only. Then a preprocessing step simply subtracts the base band from the current band to get the band difference.

$$Band_{diff} = Band_{curr} - Band_{base} \quad (1)$$

This seems to be a simple act, but leads to a lot of benefits. For example in RGB images, the bands that can be used during prediction without violating the reversibility of the algorithm are  $G$ ,  $R$ ,  $B$ ,  $R - G$ ,  $B - G$ . Instead of having three original bands, now we have five “bands” (some are difference bands) that can be used in prediction. For images with any number of bands, there always exist an original band and a difference band for encoding each band. This enables adaptation between intraband and interband prediction. Also, in this way, each band is only coupled with the base band and no multi-band joint encoding is performed. Since the base band is coded independently, it can be retrieved any time without processing other bands. Once the base band is retrieved, the current band can be retrieved. This allows the flexibility of compressing any number of bands and enables easy access to any bands. For any bands except the base band, multi-mode strategy is applied on both the original band and the difference band.

### B. Run-mode

Run-length coding is simple and efficient in grouping identical symbols [4]. It encodes the occurrence, i.e. the number of times that the symbol occurs consecutively, also called *run-length*. We use run-length coding to encode the homogeneous regions of the image. Fig. 2 shows the neighboring pixels of the current pixel  $X$  according to their geographical positions. When  $W = N = NW = NE$ , the current pixel is assumed to be in a homogeneous region and is tried to be encoded in run-mode. If  $X$  is identical to  $W$ , the run-length increases by one; otherwise “run” stops and the current run-length is encoded. The latter case means that encoding symbol in run-mode is unsuccessful, so the symbol is encoded in regular-mode.

### C. Ternary-mode

Ternary-mode is our new proposal and is inspired by the binary-mode in CALIC, which works on the binary area where there are only two different pixels in the neighborhood, e.g. black and white texts. However, unlike CALIC, our new ternary-mode targets on two types of areas – clear edge areas and smooth but not exactly homogeneous areas. Edge, which appears as the abrupt changes in pixel intensity, is very difficult to predict. Therefore, instead of predicting it, we propose to record the similarity between the edge pixels and their neighbouring pixels. In areas where a sharp edge occurs, as shown in Fig. 3a, pixels on the edge tend to be the same or similar but pixels at the two sides of the edge are usually different; also, in areas where a less sharp edge occurs, as in Fig. 3b, pixel values tend to be changing gradually from non-edge area to edge area. In both cases, we assume that within a small neighborhood of the current pixel, say the seven neighbouring pixels in Fig. 2, there are no more than three distinctive symbols and the ternary-mode is triggered. In operation, pixel  $W$  as the first unique pixel value, is represented as  $s_1$ . Then the other six pixels in the neighbourhood are evaluated and the second and third distinctive pixels are represented as  $s_2$  and  $s_3$ , respectively. By comparing the current pixel with  $s_1$ ,  $s_2$  and  $s_3$ , we can assign a value to the current pixel by

$$T = \begin{cases} 0, & \text{if } X = s_1; \\ 1, & \text{if } X = s_2; \\ 2, & \text{if } X = s_3; \\ \text{escape,} & \text{otherwise.} \end{cases} \quad (2)$$

In other word, the current pixel can be denoted by the order of its value appearance in the neighbourhood, given the condition that the checking in the neighbourhood is always conducted in the same order. “Escape” happens when the current pixel  $X$  is not equal to any of the pixel values in the neighbourhood and thus encoding in this mode fails. It is a way of switching among different modes. Fig. 3 shows the areas that the ternary-mode is performed.  $T$  indicates the symbols encoded by ternary-mode, while  $R$  indicates run-mode, and the colour is the gray-level of the symbols. The figure tells that edge areas can be largely covered by this mode.

We choose to use three distinctive pixel values but not fewer or more for the following reasons:

- 1) In the cases shown in Fig. 3, there are usually more than two distinctive pixel values in the neighbourhood. Using only two pixel values cannot adequately describe the edge conditions.
- 2) In many cases, image edges are more complicated than the ones shown in Fig. 3. However, allowing more distinctive pixel values is very likely to result in more negative than positive effect, as explained below:
  - a) It makes entering the ternary-mode too easy, if four or more different pixel values are allowed in a 7 pixel neighbourhood. This would fail to characterise the specific areas that are suitable to be encoded in ternary-mode;
  - b) It would lead to a lot more “escapes”. Because more random areas are classified as applicable in ternary-mode, the current pixel is more likely to fail to find a match with any of the pixels in a more diverse neighbourhood;
  - c) Allowing more distinctive pixel values would increase the alphabet size, and hence the bits that are needed to encode pixels.

The alphabet size for encoding in this mode is only 4 instead of 256 in the original form, so lower entropy can be obtained. Ternary-mode also works as a “backup” of the run-mode in smooth but not exactly homogeneous regions.

#### D. Regular-mode

The regular-mode is triggered, either when the entry conditions for run-mode and ternary-mode cannot be met, or when encoding in other modes fails. The regular-mode consists of intraband and inter-band prediction, which is selected according to the local features adaptively. Details of the interband prediction and switching strategy are discussed in next section.

### IV. Band Shifting and Gradient based switching

We design a simple band shifting technique for interband prediction, and adapt the GAP from CALIC [5] for intra-band prediction. However, the performance of interband prediction depends on the interband correlation. In the case of strong interband correlation, interband prediction is preferred, otherwise intra-band prediction is selected. A gradient based switching method is proposed for the selection.

#### A. Band shifting for inter-band prediction

In the regions where bands are strongly correlated, pixel changes in one band often happen in another band. For instance, Fig. 4 plots the pixel values of one line in band G and band B of the image “peppers” respectively. It is clear that the dot plot of band G has a similar trend with the dash plot of band B. We also notice that although changing in a similar trend, the difference between two bands varies from areas to areas. Thus directly subtracting band B from band G tends to result in big errors. The ideal way would be to move the base band to a position that is as close to the current band as possible so that only a small difference between the current band and the shifted base band needs to be coded. There are a lot of possible ways to predict the value for band shifting. Since band shifting is only performed when the interband correlation is high, we assume that in this case the band difference is reasonably small and varies in a regular way. Therefore, we propose to use a simple Median Edge Detector [4] to predict the band shifting value. The solid plot in Fig. 4 shows that this prediction method successfully generate a zero-mean band difference between the current band and the shifted reference band.

#### B. Gradient-based Switching

For the regular-mode in the multi-mode strategy, we use the band shifting technique for interband prediction and adopt the GAP [5] for intraband prediction. Since the performance of the two predictors varies in different regions of an image depending on the spatial and spectral correlation, it is critical to decide which predictor to use in different areas. As we aim at designing a hardware amenable scheme, complex calculation of interband correlation coefficients is not desirable. We propose a simple switching method based on the local horizontal and vertical gradients, which are calculated by

$$dh = |W - WW| + |N - NW| + |N - NE| \quad (3)$$

$$dv = |W - NW| + |N - NN| + |NE - NNE| \quad (4)$$

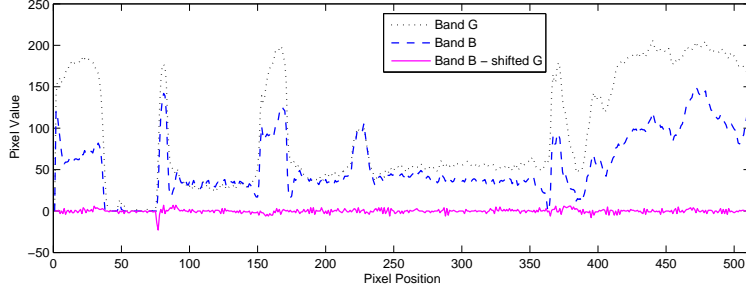


Fig. 4. Plots of one line in band G and band B and their difference after shifting

TABLE I

PROPORTIONS OF PIXELS USING INTRABAND AND INTERBAND PREDICTION AND THE RATIOS OF THE BETTER PREDICTOR IS SELECTED IN THE REGULAR MODE.

image	b_intra	b_inter	b_right_ratio	r_intra	r_inter	r_right_ratio
cmpnd1	6.41	17.66	70.13	4.62	18.64	73.33
cmpnd2	2.06	24.10	83.63	1.64	24.91	82.21
cats	1.78	47.78	87.12	1.10	47.56	90.29
water	5.33	44.19	76.53	3.04	45.49	82.15
lena	33.97	65.90	59.36	64.09	34.43	67.33
peppers	17.41	76.89	71.38	22.53	76.60	72.26
bike3	52.46	27.23	64.82	52.41	29.19	60.67
average	17.06	43.39	73.28	21.35	39.55	75.46

where  $dv$  and  $dh$  are the vertical and horizontal gradients, respectively. When calculating the interband gradients,  $W$ ,  $N$ ,  $NW$ ,  $NE$ ,  $NN$ ,  $WW$ ,  $NNE$  are substituted by the interband difference at the same positions. Interband gradients indicate how closely the two bands change in the same way. In addition to the gradients, the previous prediction error is taken into account to evaluate how well the predictor performs in the local area. Therefore, for both intraband and interband prediction, we calculate the switching coefficient  $S$  by

$$S = dv + dh + |e_w| \quad (5)$$

where  $e_w$  means the prediction error at position  $W$ . The predictor that gives smaller  $S$  is selected to encode the current pixel. We counted the proportions of pixels that are treated by intraband and interband prediction in the regular-mode respectively, in band B and R on a set of RGB images in Table I. We also calculated how often the predictor that gives smaller errors is selected, as `right_ratio`. The proportions of intraband and interband prediction do not sum up to 1 because the rest pixels are processed by the run-mode or ternary-mode. On average, more than 40% interband prediction is selected, meaning that there is a substantial amount of interband redundancy. The simple gradient-based switching technique has achieved over 70% correct choice in selecting a better predictor.

### C. Adaptation in Run-mode and Ternary-mode

The above gradient-based switching is not only used in selecting the intraband and interband prediction in regular-mode, but is also modified to be used in enabling adaptation in the run-mode and ternary-mode. Since the run-mode encodes pixels directly and the ternary-mode only records the similarity among pixels, there is no prediction error generated by these two modes. Therefore, we eliminate the term of error from Equation (5) to obtain an adaptation coefficient  $S'$ .

In the run-mode, when run-length is 0, either the pixels in the current band or in the band difference is selected according to which neighbourhood gives a smaller  $S'$ . The selected pixels are used in the run-mode and a flag is used to indicate this selection. When run-length is not 0, the previously used pixel values - whether from the current band or the band difference, are used to keep the continuity of the run.

In the ternary-mode, the whole neighbourhood of pixels used for ternary-mode are selected either from the current band or the band difference based on the value of  $S'$ . Since the coefficient  $S'$  can be calculated before receiving the current pixel, it is guaranteed that the current pixel used for comparing with its neighbouring pixels is from the same source. This adaptation in run-mode and ternary-mode improves the spatial and spectral decorrelation performance of our proposed scheme in our experiments.

We show in Table II the effect of using the original band, difference band or the two combined in the run-mode and ternary-mode. The the “adaptation” on the fourth column means choosing the bands adaptively. The resulting bit rates vary for different images, but on average, using the adaptation technique slightly improves the compression ratios.

TABLE II  
COMPRESSION RATIOS COMPARISON ON LMMIC USING DIFFERENT NEIGHBOURHOODS IN THE RUN-MODE AND  
TERNARY-MODE, IN BITS PER PIXEL

image	current band	difference band	adaptation
cmpnd1	1.117	1.054	1.057
cmpnd2	1.037	0.972	0.969
cats	1.813	1.822	1.823
water	1.434	1.436	1.442
lena	4.233	4.230	4.233
peppers	3.339	3.363	3.356
bike3	4.274	4.353	4.289
average	2.464	2.461	2.453

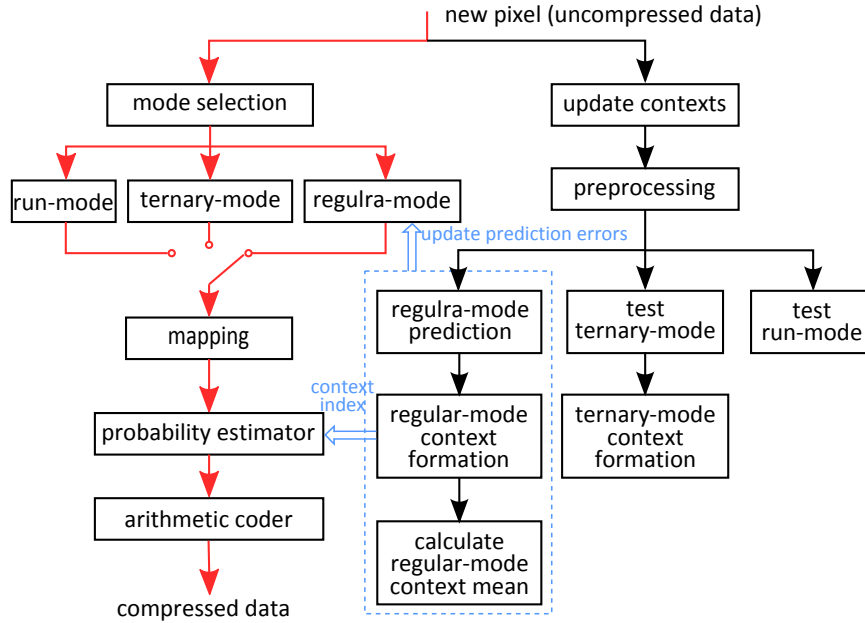


Fig. 5. Data Flow of the prediction and context modeling module

## V. HARDWARE ARCHITECTURE

We concern about the hardware amenability of the proposed algorithm for potential practical applications, especially for space application. Therefore, as previously described, LMMIC only involves a limited number of addition and shifting, and memory usage is strictly controlled. In this section we propose a suitable hardware architecture to support the proposed compression scheme. The architecture can be mainly divided into two parts – lossless image modelling and encoding. The encoding part, which includes probability estimator and binary arithmetic coder, can be found in [18]. We will only discuss the modelling part in details below.

Lossless image modelling here serves both gray-scale and multispectral images. The user can specify which category the input image belongs to. The data flow of the image compression scheme is shown in Fig. 5.

To optimise the speed and hence the throughput, the data flow of the scheme is designed as two pipelines running in parallel, as shown in Fig. 5. Line 1, indicated by the flow on the left in red, operates for the current symbol. It takes in the input symbol and selects the suitable mode to encode it. The mean of errors and context index calculated from Line 2 are fed into the multi-mode prediction and probability estimator. The output from the multi-mode prediction, which is either the “runs” of the symbols, or the symbol order from the ternary mode, or the prediction error from the regular mode, are used to drive the probability estimator and arithmetic coder. Line 2, indicated by the flow on the right in black, works for the next symbol. It takes the input symbol to update the contexts, and calculate the prediction value and context index under the selected mode for the next symbol. The advantage of dividing the procedure into two parallel pipelines is, while not violating the sequential constraint, to halve the execution time and hence obtain higher throughput. A summary of the operations in each pipelines is as follow.

TABLE III

COMPRESSION RATES COMPARISON ON SELECTED GENERAL IMAGE COMPRESSION SCHEMES, IN BITS PER PIXEL PER BAND.

image	JPEG2000	CALIC	IB-CALIC	SICLIC	LMMIC
cmpnd1	1.44	1.21	1.02	1.12	1.06
cmpnd2	1.30	1.22	0.92	0.97	0.97
cats	1.75	2.49	1.81	1.85	1.82
water	1.41	1.74	1.51	1.45	1.44
lena	4.53	4.40		4.46	4.23
peppers	3.41	4.62		3.25	3.36
bike3	5.17	4.21		4.41	4.29
<b>average</b>	<b>2.72</b>	<b>2.84</b>		<b>2.50</b>	<b>2.45</b>
park	5.72	5.39			5.30
baltic-sea-bloom (ESA)	2.84	3.35			2.74

**Line 1:**

- 1) Select a suitable mode and calculate prediction error  $\epsilon = X - (\hat{X} + error\_mean)$ ;
- 2) Update the sum of errors *sum* and the number of pixels *count* in each context;
- 3) Map prediction error  $\epsilon$  to  $\tilde{\epsilon}$ ;
- 4) Update coding context index  $Q$ ;
- 5) Encode the prediction error with probability estimator and arithmetic coder.

**Line 2:**

- 1) Update contexts with new symbol;
- 2) Calculate primary prediction value  $\hat{X}$  for regular mode, and evaluate the condition of entering run-mode and ternary-mode;
- 3) Calculate the texture pattern;
- 4) Calculate the error energy and the context index;
- 5) Calculate the mean of the errors *error\_mean*.

**VI. PERFORMANCE COMPARISON**

We carried out experiments to compare the compression ratios of LMMIC and some state-of-the-art schemes on a set of colour images and space images from the European Space Agency (ESA) image database. We choose a set of standard ISO 3-band RGB images, a 4-band CMYK image “park” and a RGB satellite image of “baltic-sea-bloom” (courtesy ESA) as test images. The RGB images include continuous-tone images, compound images and synthetic images. We compare LMMIC with JPEG2000 [19], intra-band CALIC [5], Inter-band CALIC (IB-CALIC) [12] and SICLIC [13]. JPEG-2000 is the current image compression standard using wavelet. IB-CALIC is an extension of the benchmark compression scheme CALIC and uses the CALIC algorithm across different spectral bands. SICLIC is a simple colour image compression scheme based on LOCO [4]. The results of IB-CALIC and SICLIC are extracted from [13]. Some results are absent here due to the unavailability of the programs. Table. III shows that our proposed scheme outperforms JPEG2000 and intra-band CALIC by 10% and 14%, respectively. It is superior than SICLIC on average, though slightly inferior than IB-CALIC which has higher computational complexity. It also has better compression ratio on image “park” and “baltic-sea-bloom” than JPEG2000 and CALIC.

Lossless compression of space image is one of the main concerns of LMMIC. We use the 8-bit CCSDS test image set, downloaded from the CCSDS website [20]. Among them, “coastal” is a LANDSAT 7 image; “europa3” is the Galileo image from Europa; “marstest” is from the Mars Pathfinder; “lunar” is a Galileo image; “spot-la\_b3” and “spot-la\_panchr” are SPOT 3 images. As LMMIC is intended for hardware implementation and high-speed spaceborne application, test results relevant for this purpose are presented. We compare LMMIC with some state-of-the-art low complexity schemes. CCSDS is the current Recommendation for space image compression; PRDC [21] is the CCSDS Rice coder; JPEG-LS [22] is the lossless image compression standard; SPIHT [9] is a wavelet-based progressive image compressor; ICER [23] is another progressive wavelet-based image compressor, whose software implementation is used in Mars Exploration Rover missions for on-board lossy image compression. For CCSDS and JPEG2000, when strip-based or frame-based options are available for these algorithms, the better frame-based ones are chosen in this comparison, but the frame-based option has a higher memory requirement. Our proposed method should only require memory as little as that for strip-based algorithms. Table. IV shows the compression results of all these algorithms in bit rates on the test images. Results of all the algorithms except ours are extracted from [24]. The proposed LMMIC achieved better compression than other algorithms in comparison by between 15% and 2% in terms of bit rates.

Overall, the proposed lossless multi-mode multispectral image compression (LMMIC) scheme achieves very good compression ratios compared with state-of-the-art compression schemes on the colour test images and space test images. Since the inter-band coding in LMMIC only couples two bands, it enjoys the flexibility of compressing images with any number of bands and easy access to any bands. This is important for the proposed algorithm to be applied on various images types, especially on multispectral space images. Moreover, it has low complexity since it requires a small number of simple operations such as addition, shifting and two-way comparison.

TABLE IV

COMPRESSION RATES COMPARISON ON SELECTED SPACE IMAGE COMPRESSION SCHEMES, IN BITS PER PIXEL PER BAND

image	CCSDS	PRDC	JPEG-LS	JPEG2000	SPIHT	ICER	proposed
coastal_b1	3.36	3.56	3.09	3.13	3.09	3.07	3.00
coastal_b2	3.22	3.32	2.90	2.97	2.94	2.92	2.84
coastal_b3	3.48	3.68	3.22	3.23	3.21	3.20	3.14
coastal_b4	2.81	2.91	2.41	2.53	2.57	2.55	2.37
coastal_b5	3.16	3.30	2.81	2.94	2.91	2.89	2.79
coastal_b6h	3.02	2.75	2.50	2.60	2.71	2.54	2.52
coastal_b6l	2.35	2.03	1.76	1.96	2.02	1.87	1.84
coastal_b7	3.45	3.66	3.17	3.22	3.17	3.15	3.10
coastal_b8	3.66	3.93	3.42	3.40	3.35	3.31	3.28
europa3	6.61	7.48	6.64	6.52	6.46	6.30	6.42
marstest	4.78	5.39	4.69	4.74	4.64	4.63	4.60
lunar	4.58	5.23	4.35	4.49	4.43	4.40	4.20
spot-la_b3	4.80	5.20	4.53	4.69	4.70	4.56	4.43
spot-la_panchr	4.27	4.87	4.00	4.13	4.11	4.03	3.90
average	3.82	4.09	3.54	3.61	3.59	3.53	3.46

## VII. CONCLUSIONS

An original Lossless Multi-Mode Interband image Compression (LMMIC) scheme is proposed. The concept of segmentation is well ingrained in this scheme to encode different regions in the image using different methods adaptively. The simple and efficient band shifting technique and the switching strategy successfully remove the interband redundancy. Experiments show that LMMIC achieves highly competitive compression ratios and provides the merits of compressing any number of bands as well as easy access to any bands, which are not offered by many other schemes. The complexity of the scheme is strictly constrained and hardware amenability is maintained. A corresponding hardware architecture is also proposed to support the functionality of the proposed algorithm.

## REFERENCES

- [1] Visual arts system for archiving and retrieval of images. <http://users.ecs.soton.ac.uk/km/projs/vasari/>. National Gallery.
- [2] The landsat program. <http://landsat.gsfc.nasa.gov/>. National Aeronautics and Space Administration.
- [3] Airborne visible/infrared imaging spectrometer (aviris). <http://aviris.jpl.nasa.gov/>. Jet Propulsion Laboratory, California Institute of Technology.
- [4] M. J. Weinberger, G. Seroussi, and G. Sapiro, "LOCO-I: A low complexity, context-based, lossless image compression algorithm," in *Proc. Data Compression Conference*, Mar. 1996, pp. 140–149.
- [5] X. Wu and N. Memon, "Context-based, adaptive, lossless image coding," *IEEE Trans. Commun.*, vol. 45, no. 4, pp. 437–444, Apr. 1997.
- [6] A. Said and W. A. Pearlman, "A new fast and efficient image codec based on set partitioning in hierarchical trees," *IEEE Trans. Circuits Syst. Video Technol.*, vol. 6, no. 3, pp. 243–250, Jun. 1996.
- [7] J. Mielikainen and P. Toivanen, "Improved vector quantization for lossless compression of AVIRIS images," in *Proc. XI European Signal Process. Conf.*, Sep. 2002.
- [8] G. Motta, F. Rizzo, and J. A. Storer, "Compression of hyperspectral imagery," in *Proc. Data Compression Conf.*, Mar. 2003, pp. 333–342.
- [9] P. Dragotti, G. Poggi, and A. Ragozini, "Compression of multispectral images by three-dimensional SPIHT algorithm," *IEEE Trans. Geosci. Remote Sens.*, vol. 38, no. 1, pp. 416–428, Jan. 2000.
- [10] X. Tang, W. A. Pearlman, and J. W. Modestino, "Hyperspectral image compression using three-dimensional wavelet coding," in *Proc. SPIE*, vol. 5022, Jan. 2003, pp. 1037–1047.
- [11] A. Benazza-Benyahia, J. C. Pesquet, and M. Hamdi, "Vector-lifting schemes for lossless coding and progressive archival of multispectral images," *IEEE Trans. Geosci. Remote Sens.*, vol. 40, no. 9, pp. 2011–2024, Sep. 2002.
- [12] X. Wu and N. Memon, "Context-based lossless interband compression – extending CALIC," *IEEE Trans. Image Processing*, vol. 9, no. 6, pp. 994–1001, 2000.
- [13] R. Barequet and M. Feder, "SICLIC: a simple inter-color lossless image coder," in *Proc. Data Compression Conference, DCC'99*, Mar. 1999, pp. 501–510.
- [14] S. R. Tate, "Band ordering in lossless compression of multispectral images," *IEEE Trans. Comput.*, vol. 46, no. 4, pp. 477–483, Apr. 1997.
- [15] B. Meyer and P. E. Tischer, "TMW - a new method for lossless image compression," in *Proc. Picture Coding Symp.*, Oct. 1997.
- [16] L. Shen and R. M. Rangayyan, "A segmentation based lossless image coding methods for high-resolution medical image compression," *IEEE Trans. Med. Imag.*, vol. 16, no. 3, pp. 301–307, Jun. 1997.
- [17] K. Ratakonda and N. Ahuja, "Lossless image compression with multiscale segmentation," *IEEE Trans. Image Processing*, vol. 11, no. 11, pp. 1228–1237, Nov. 2002.
- [18] J. Nunez-Yanez and V. Chouliaras, "A configurable statistical lossless compression core based on variable order Markov modeling and arithmetic coding," *IEEE Trans. Comput.*, vol. 54, no. 11, pp. 1345–1359, 2005.
- [19] D. S. Taubman and M. W. Marcellin, *JPEG2000 Image Compression Fundamentals, Standards and Practice*. Norwell, MA: Kluwer, 2002.
- [20] "CCSDS documents," <http://cwe.ccsds.org/sls/docs/sls-dcl/>, The Consultative Committee for Space Data Systems (CCSDS).
- [21] R. Vitulli, "PRDC: An ASIC device for lossless data compression implementing the Rice algorithm," in *Proc. IEEE Int. Geoscience and Remote Sensing Symp.*, vol. 1, 2004, pp. 317–320.
- [22] M. Weinberger, G. Seroussi, and G. Shapiro, "The LOCO-I lossless image compression algorithm: Principles and standardization into JPEG-LS," *IEEE Trans. Image Processing*, vol. 9, no. 8, pp. 1309–1324, Aug. 2000.
- [23] A. Kiely and M. Klimesh, "The ICER progressive wavelet image compressor," IPN Progress Report 42-155, Jet Propulsion Laboratory, California, US, Tech. Rep., 2003.
- [24] "Report concerning space data system standards," Information Report, CCSDS 120.1-G-1, Green Book, The Consultative Committee for Space Data Systems (CCSDS), Washington, DC, USA, Tech. Rep. 1, Jun. 2007.